buildings

Article

Cascaded Control for Building HVAC Systems in Practice

Chris Price [1], Deokgeun Park [2] and Bryan P. Rasmussen [2,*]

[1] Oak Ridge National Laboratory, Oak Ridge, TN 37830, USA
[2] J. Mike Walker '66 Department of Mechanical Engineering, Texas A&M University, College Station, TX 77840, USA
* Correspondence: brasmussen@tamu.edu

Abstract: Actuator hunting is a widespread and often neglected problem in the HVAC field. Hunting is typically characterized by sustained or intermittent oscillations, and can result in decreased efficiency, increased actuator wear, and poor setpoint tracking. Cascaded control loops have been shown to effectively linearize system dynamics and reduce the prevalence of hunting. This paper details the implementation of cascaded control architectures for Air Handling Unit chilled water valves at three university campus buildings. A framework for implementation the control in existing Building Automation software is developed that requires only a single line of additional code. Results gathered for more than a year show that cascaded control not only eliminates hunting in control loops with documented hunting issues, but provides better tracking and more consistent performance during all seasons. A discussion of efficiency losses due to hunting behavior is presented and illustrated with comparative data. Furthermore, an analysis of cost savings from implementing cascaded chilled water valve control is presented. Field tests show 2.2–4.4% energy savings, with additional potential savings from reduced operational costs (i.e., maintenance and controller retuning).

Keywords: building; HVAC; control; energy efficiency; faults

Citation: Price, C.; Park, D.; Rasmussen, B.P. Cascaded Control for Building HVAC Systems in Practice. *Buildings* **2022**, *12*, 1814. https://doi.org/10.3390/buildings12111814

Academic Editor: Etienne Saloux

Received: 1 September 2022
Accepted: 10 October 2022
Published: 28 October 2022

1. Introduction

Actuator hunting is a known and well documented problem in the HVAC field affecting a wide range of systems from vapor compression systems to Variable Air Volume (VAV) terminal units. Hunting is an undesired oscillation in a system's control input due only to the interaction of the controller with the system dynamics, in contrast to oscillations due to a changing external input. The phenomenon is the result of nonlinear and time varying dynamics associated with HVAC systems. For example, VAV units have steady-state input/output gains that can vary by more than an order of magnitude over the full range of operating conditions [1]. Fixed controllers will struggle to provide consistent performance when a system operates far from its tuning conditions. Hunting can also be spread to upstream and downstream components in an HVAC system, making identification of the root cause difficult. A survey at Texas A&M University showed campus Air Handling Units displayed high levels of hunting, with chilled water valves hunting 70% and supply fans hunting nearly 25% of operating time [2].

While hunting is often easily identifiable by visual inspection of a measured signal, there are several automated methods to detect the behavior. These methods are able to distinguish between daily disturbances such as outdoor air temperature and the high frequency oscillations that stem from the controller. The time between consecutive zero crossings of the Integrated Absolute Error signal is used to detect the presence of oscillations [3]. Hunting is detected when two or more crossings occur far enough apart and with sufficient magnitude. This paper uses the simple method proposed by [2] to identify and measure hunting times. This method only requires the input signal and uses the magnitude and time between consecutive sign changes to identify hunting. For details on the algorithm parameters and implementation, see [4].

Most control loops utilized in the HVAC field are Proportional-Integral-Derivative (PID) controllers. As shown in Equation (1), PID is a low order controller consisting of three parts that respond to instantaneous error (P), steady-state error (I), and changes in error (D). Despite its simplicity, PID has proven versatility and robustness for controlling a wide range of systems in many fields [5–7]. In many HVAC applications, the time derivative 'D' term is not used due to its sensitivity to noise and additional implementation complexity. For effective operation, the control gains, k_p, k_i, and k_d must to be tuned for the equipment and operating conditions. There are numerous methods for tuning PID controllers each with their own unique goals and procedures [8]. The most common of which are the methods of Ziegler and Nichols. Building Automation System (BAS) software often have built-in PID functions that implement the controller with native anti-windup and saturation solutions. Such commands typically have recommended initial gains from which the tuning process can begin. Further background on PID control can be found in [7,8].

$$\text{PID}(t) = k_p e(t) + k_i \int_0^{\infty} e(t)\, dt + k_d \frac{d}{dt} e(t), \tag{1}$$

The tendency for HVAC systems to have large, load-dependent nonlinearities often causes difficulties for PID controllers; see [1] for examples. Nonlinearities are the result of fundamental heat transfer processes and system actuators that typically do not have linear flow profiles. PID controllers tuned in high system gain conditions will have very slow response times when operating conditions change. Conversely, a controller tuned in low gain conditions can easily develop hunting behavior as system gains increase. These variations in performance lead to hunting behavior and decreased system efficiency. To address such issues, some have focused on assessing poor control and designed control quality factors (CQF) to analyze control performance based on measured data [9].

Improving the control of HVAC subsystems is important for two main reasons. First, the nonlinear power profiles of actuators such as fans or pumps (Equation (2)) causes overall energy use and operational costs to increase with oscillatory (hunting) behavior. Second, hunting behavior increases actuator wear and, finally, system-level coordinating controllers, such as Model Predictive Control (MPC), are increasingly used to optimize system setpoints. These supervisory controllers depend on subsystem controllers that can consistently track setpoints. Hunting can also interfere with model predictions, reducing the effectiveness of advanced control techniques and resulting in lost efficiency.

$$\frac{P_1}{P_2} = \left(\frac{\omega_1}{\omega_2}\right)^3, \tag{2}$$

This paper details the implementation of cascaded control architectures for building Air Handing Unit (AHU) temperature control. Research has shown that cascaded control loops are an effective strategy to reduce common HVAC issues stemming from nonlinear dynamics and input/output coupling, including the elimination of hunting behavior. The proposed architecture uses nested PID control loops to improve system performance by isolating and linearizing system dynamics. Cascaded loops are inherently low order and easily implementable in existing Building Energy Management (BEM) software. As will be shown, this approach requires no special software commands and can be implemented with a single line of additional code, facilitating adoption in HVAC applications.

The simplest embodiment of a cascaded control architecture is the addition of a proportional control loop inside of a standard Proportional-Integral (PI) controller. An example of this approach, would be the representation of a cascaded control loop applied to nonlinear system, as seen in Figure 1. The nonlinear plant is represented as a Hammerstein model consisting of a nonlinear gain function dependent on operating condition 'σ' and some dynamic of unitary gain. In this model, inner and outer loop signals (y_i and y_o) and nonlinearities (ψ_i and ψ_o) can be equal or unique. Note that the plant nonlinearity is contained inside the inner loop control where it is effectively linearized by proportional feedback with gain k_L. This affect can be seen in Equation (3), where the inner and outer loop nonlinearities are placed in the numerator and denominator of the inner loop transfer function. This structure allows nonlinearities to counteract themselves over all operating conditions and thereby reducing their overall effect. Additionally, the inner loop process will essentially become a static gain as the inner loop gain becomes large. If the nonlinearities are equal or multiplicatively related, all dependence on operating condition is eliminated. This behavior is guaranteed if both $\psi_i(\sigma)$ and $\psi_o(\sigma)$ are monotonic and share the same trends. For more details on cascaded control and properties of the inner loop gain, see [10].

$$L(s, k_L, \sigma) = \frac{k_L \psi_o(\sigma) G_o(s)}{1 + k_L \psi_i(\sigma) G_i(s)}, \tag{3}$$

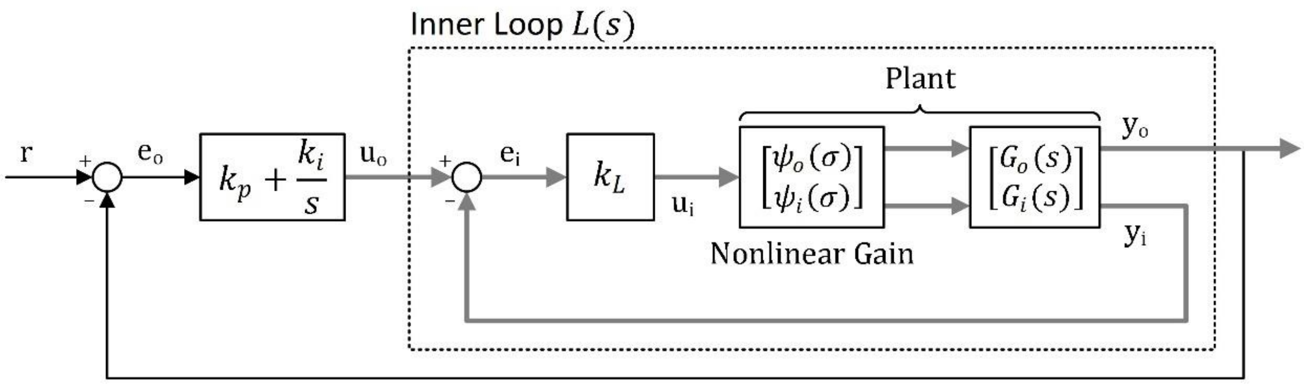

Figure 1. Block diagram of a generalized cascaded control loop. Subscripts 'i' and 'o' denote the inner and outer loops, respectively.

Recent work with cascaded control architectures has shown it to be an effective strategy for control of a wide range of HVAC systems. Simulations have improved control of and eliminated hunting behavior in VAV units, hydronic radiator systems, and AHUs [1]. The architecture was also able to decouple the dynamics of a multi-evaporator refrigeration systems and improve individual tracking performance [11]. Although cascaded loops require an additional control loop and a more complex tuning process, simple metrics have been developed to quantify the benefits of cascaded control and tune inner and outer loop gains accordingly along with optimal frameworks [10] and simple tuning rules [12].

The linearization and decoupling effects of cascaded control are particularly important for Model Predictive Control algorithms that rely on consistent and linear sub-system behavior. The simplicity of cascaded controllers can enable MPC algorithms to better optimize building HVAC performance while still guaranteeing control stability. Neither MPC nor cascaded control, however, has seen widescale testing in real building systems. Numerous studies have implemented cascaded controllers in simulation with simple models of HVAC systems or with experimental test rigs [13]. In [14], a Hybrid Expansion Valve (HEV) was used to linearize the response of a small laboratory vapor compression cycle system. The HEV used a combination of physical and digital feedback to implement the cascaded control loop and eliminate differences in high flow and low flow conditions. Cascaded control has also appeared in trade manuals [15] that adjust equipment exit temperatures based on room temperature setpoint errors. These manuals, however, do not focus or test the linearization behavior of the architecture. Testing of MPC controllers in buildings has similarly been mostly in simulation [16] with some studies beginning to test on real building systems [17].

This paper presents results of a widescale implementation of cascaded control loops for AHU discharge air temperature control in three university campus buildings (9 AHUs). These controllers regulated the position of chilled water supply valves and utilized standard building automation software. The implementation required the addition of only a single line of code to existing control routines. Data was collected over multiple years, comparing building operation under existing control algorithms, and the proposed cascaded control approach. A comparative analysis of this data is presented, including the primary source of wasted energy and costs for discharge air temperature control. The results lay the groundwork for future work testing the implementing of an MPC algorithm across a whole building HVAC system.

2. Materials and Methods

Most building automation software can implement PID control loops using a built-in command. Consider, for example, a LOOP command given below that has 11 usable inputs. These inputs define the direction of control (type = 0 direct control, type = 1 indirect), the regulated signal (pv), the control signal (cv), the setpoint signal (sp), PID control gains (pg, ig, and dg), sample time (st), loop bias, and the saturation limits of the controller (lo and hi). Loop gains have a divisor (usually 1000) and have recommend values such as pg = 1000 and ig = 20 that provide good control for a wide range of systems. A sampling of AHUs at Texas A&M reveals that most PI control loops have these standard values, which strongly indicates that many loops operate with factory defaults and may never receive additional tuning unless problems are detected [4]. The relationship between LOOP gains and a standard PI control formulation is given in Equation (4) where it is important to note the multiplication of the sampling time and integral gain.

$$\begin{aligned} &\mathrm{LOOP}(\text{type, pv, cv, sp, pg, ig, dg, st, bias, lo, hi, } 0) \\ &u = k_p \cdot e + k_i t_s \cdot \sum e = \tfrac{\mathrm{pg}}{1000} \cdot e + \tfrac{\mathrm{ig}}{1000} t_s \cdot \sum e, \end{aligned} \tag{4}$$

A first pass implementation of a cascaded control loop in building software is given by Algorithm 1 for a discharge air temperature controller. Note that the inner and outer loops are implemented using two LOOP commands and an intermediate virtual point named 'AHU.DATLOOP1.ILSP' (Discharge Air Temperature Loop 1, Inner Loop Set Point) that stores the inner loop setpoint signal (i.e., the outer loop output). Although most LOOP commands in building software will have built-in saturation and anti-windup solutions, the interaction of the two loops must be considered. When the inner loop output (i.e., valve position) becomes saturated, the outer loop controller must also be disabled to avoid windup while the inner loop is disabled. Lines 6 through 7 deal with this issue by checking if the inner loop signal is saturated and then dynamically enabling/disabling the outer LOOP command on Line 11 accordingly. Although intuitive, this code is somewhat lengthy, requires the creation of intermediate virtual points, and has seven tunable variables.

Algorithm 1 Cascaded control implementation with two LOOPs

```
1:  C Point Name Abbreviations
2:  DEFINE(X,"AH01.")
3:  DEFINE(Y,"DATLOOP1.")
4:  DEFINE(Y,"DATLOOP2.")
5:  C Outer Loop Anti-Windup
6:  IF("%X%CCV" .GT. 1 .AND. "%X%CCV" .LT. 99) THEN SET(0,SECND2)
7:  IF(SECND2 .GT. "DISABLE.TIMER") THEN DISABL(110) ELSE ENABLE(110)
8:  C Inner Loop Control
9:  LOOP(128,"%X%DAT","%Y%ILSP","%X%DAT.S","%Y%P","%Y%I",0,"%Y%TIME","%Y%BIAS",50,70,0)
10: C Outer Loop Control
11: LOOP(0,"%X%DAT","%X%CCV","%Y%ILSP","%Z%P",0,0,"%Z%TIME","%Z%BIAS",50,70,0)
```

An alternative approach to cascaded control can shorten the code required and simplify implementation. Consider the inner loop control signal given in Equation (5) where $e_1 = r - y_1$, $e_2 = u_1 - y_2$, B_1, and B_2 are outer and inner loop errors and biases, respectively. Note that the first two terms resemble the output of a PI controller with PI gains of $k_L k_p$ and $k_L k_i$ while the final terms are a combination of loop biases and inner loop feedback.

$$\begin{aligned} u_2 &= k_L e_2 + B_2 \\ &= k_L(u_1 - y_2) + B_2 \\ &= k_L\left[\left(k_p e_1 + k_i \sum e_1 + B_1\right) - y_2\right] + B_2 \\ &= k_L k_p (r - y_1) + k_L k_i \sum (r - y_1) + B_2 + k_L B_1 - k_L y_2, \end{aligned} \tag{5}$$

Expressed in this form, the cascaded controller can clearly be implemented as a *single* LOOP command without the need for the extra intermediate virtual point as before. This is important because inner/outer loop anti-windup issues are avoided as the new algorithm takes advantage of built-in saturation features. Code based on this implementation for AHU control is given by Algorithm 2 taking into account that the outer and inner loops are reverse and direct acting, respectively. The bias term is calculated and stored in a local variable $LOC1 on Line 4 because some software does not allow for calculations inside of function calls. Note that the simplified code eliminates fives lines and reduces the number of tuning variables to five. One disadvantage of this implementation is the loss of ability to have different sampling times for the inner and outer loops. Despite this, all benefits of cascaded control can still be realized even through the two loops operate at the same sampling rate.

Algorithm 2 Simplified cascaded control implementation with one LOOP

```
1: C Point Name Abbreviation
2: DEFINE(X,"AH01.")
3: C Bias Term Calculation
4: $LOC1 = "%X%BIAS" + "%X%KL"*"%X%DAT"
5: C Cascaded Control
6: LOOP(0,"%X%DAT","%X%CCV","%X%DAT.S","%X%P","%X%I",0,"%X%TIME",$LOC1,0,100,0)
```

The final sections of this paper detail results of applying cascaded control within three campus buildings. Details about the size, layout, and location of each building will be provided as well as comparisons between original PI and cascaded control. Finally, a discussion of the cost of poor AHU control is presented with a savings estimate based on observed performance improvements.

3. Results

Working with the staff at the Utilities and Energy Services, limited access to the HVAC control systems of Building 1497, 0474 and 1600 was established.

3.1. Building 1497 Results

This building is a single-story, rectangular building with an area of 12,040 ft^2 (1119 m^2) and consisting of ten temperature-controlled zones and one unconditioned server room with the general floor plan shown in Figure 2. The building is serviced by a 14 ton single rooftop AHU consisting of a chilled water coil with valve, return/outdoor air dampers, and variable speed fan capable of suppling 6425 CFM of air. The unit has two sensors for discharge air temperature and end static pressure. Zones 1–10 have VAV terminal boxes equipped with a hot water reheat coil and an air damper. The hot and cold water needs of the building are serviced by two dedicated loops that provide access to the university's centralized heating and cooling water supply.

Building 1497 uses a complex, nested PI-based architecture for its HVAC control (Figure 3). During normal operation, PI controller (1) modulates the speed of the supply fan to maintain static pressure in the air ducts. The End Static Pressure (ESP) setpoint is the output of another PI controller (2) that compares the damper demand given by Equation (6) to a design setpoint $D_{set} = 60$. Room air temperature is regulated by a cascaded damper control architecture similar to the one discussed in [1]. An outer loop PI controller (3) uses room temperature error to calculate a flow demand $F_i \in [0, 100]$ that determines the flow rate required for each room. Flow demand is converted to a flow rate though linear interpolation between minimum ventilation requirements and the maximum system output. Inner loop control (4) uses local control and a flow rate sensor to match the outer loop flow setpoint. Similar to ESP control, the AHU discharge air temperature setpoint is generated by a PI controller (5) using the cooling demand calculation of Equation (7) and the design setpoint $C_{set} = 60$. PI controllers (6–7) modulate hot and cold-water supply valves to match the exit/supply air temperature setpoint.

$$D = \frac{3}{5}\max(\theta_i) + \frac{2}{5}\left(\frac{1}{n}\sum_{i=1}^{n}\theta_i\right), \tag{6}$$

$$C = \frac{3}{5}\max(F_i) + \frac{2}{5}\left(\frac{1}{n}\sum_{i=1}^{n}F_i\right), \tag{7}$$

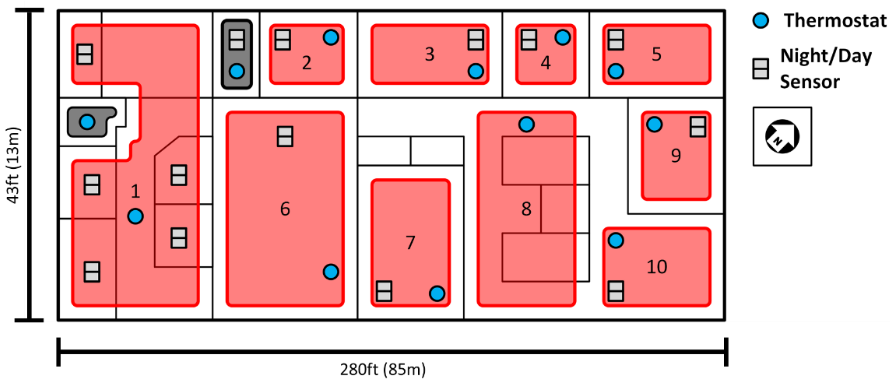

Figure 2. Layout of HVAC zones for Building 1497.

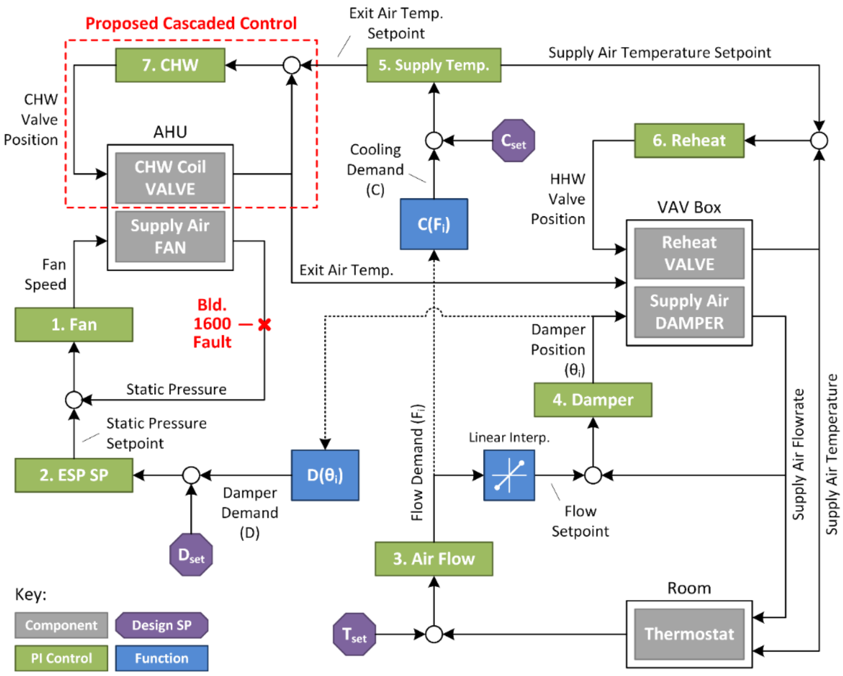

Figure 3. HVAC control system diagram for Building 1497.

Chilled water valve control used to regulate AHU exit air temperature for Building 1497 has documented issues with actuator hunting. Oscillations are most pronounced during low load conditions such as early morning or during cool winter weather. For example, the valve hunted 57% of its operating time during the three-month period of 1 November 2013 to 1 February 2014 while the valve hunted only 14% from 1 May to 1 August 2016. PI valve control has three distinct hunting behaviors as seen in Figure 4.

Under high load, valve control typically does not hunt (19 March 2016). In early spring, temperatures are usually warm in the afternoon but cool in the evening resulting in hunting late in the day (23 March 2016). On other spring days, there is never enough load to prevent hunting behavior (30 March 2016). This behavior indicates that control performance is strongly tied to the operating conditions of the system.

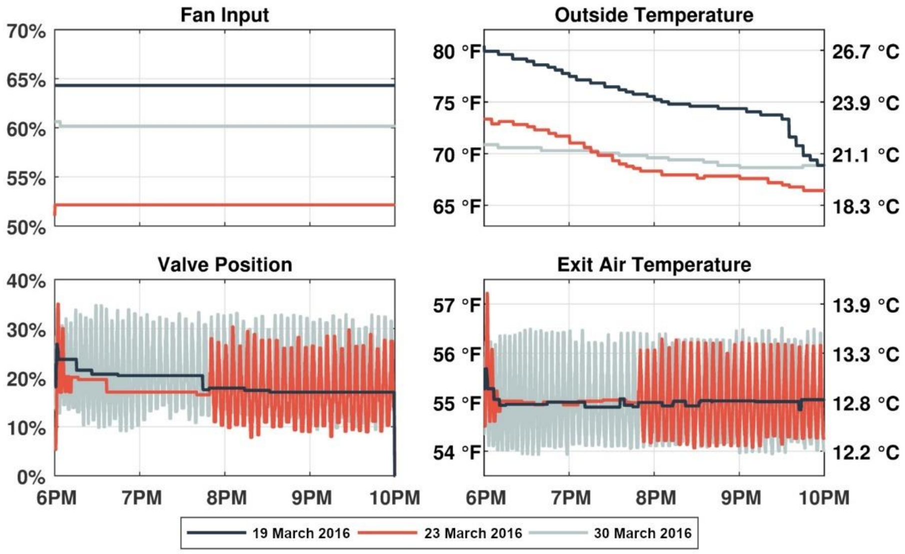

Figure 4. Building 1497 PI control performance displays three hunting behaviors depending on system load (outside temperature). The chilled water valve will not hunt, hunt late in the day, or hunt continuously.

Cascaded control was applied to Building 1497 chilled water valve control from approximately October through December of 2015. Testing utilized Algorithm 1 with gains tuned using step identification tests for a range of supply fan speeds (system loads) from 20–90%. Cascaded gains of $k_L = 4$, $k_{pc} = 1.25$, and $k_{ic} = 0.2$ were chosen using the analysis and the tuning procedure from [10]. Figure 5 shows that valve hunting modes seen with the original PI control for a range of system loads has been eliminated without sacrificing performance.

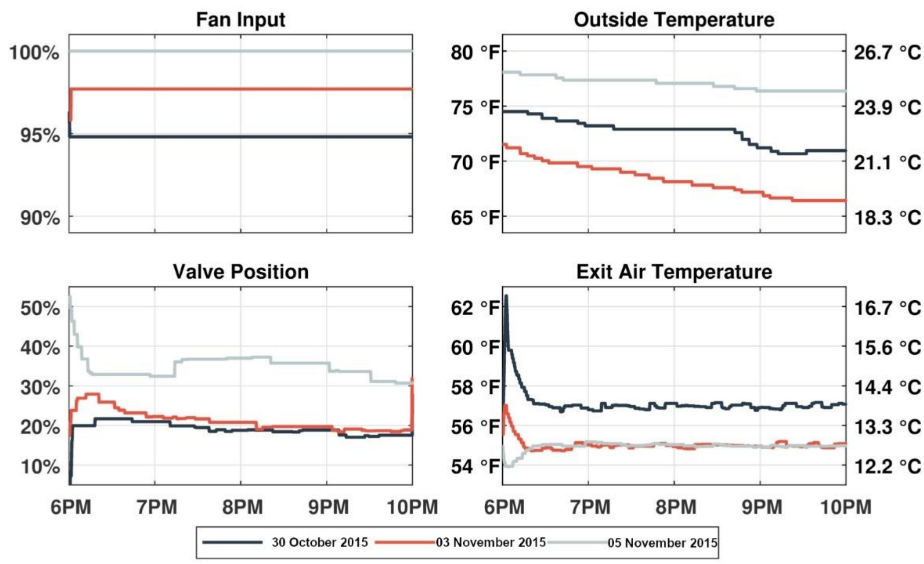

Figure 5. Building 1497 cascaded control performance displays no hunting behavior over a range of system loads.

3.2. Building 0474 (Philosophy Department) Results

Building 0474 is a four-story building originally completed in 1914 that houses the university Philosophy Department. A total renovation in 2012 included upgrading the entire HVAC system and controls. Each floor has a dedicated AHU for the floor and is numbered for the floor it covers. AHU1, AHU2, AHU3 and AHU4 have capacities of 35, 27, 21 and 22 tons and total air flow capacity of 12,000, 10,000, 8000, and 8000 CFM, correspondingly. Building 0474 has approximately 54000 ft^2 (5017 m^2) of office space with approximately 20 heating and cooling zones per floor, controlled by the AHU in the middle of the floor area (Figure 6). Each floor has its own AHU where return and outside air are mixed and conditioned. Zones have a parallel fan powered VAV terminal box with hot water reheat coil and return air ducting that draws warm air from the ceiling plenum for 'free' reheat. The heating coil can be used for substitute reheat when at the minimum supply air flow rate. The building control system has a wide array of sensors including relative humidity, CO_2, and outside air flow rate (ventilation). The overall temperature control structure is the same as at Building 1497 (Figure 3) with the exception of additional complexity due to the upgraded terminal boxes and ventilation sensors.

Figure 6. Layout of HVAC zones and exterior of Building 0474.

Cascaded control Algorithm 2 was initially tested on the fourth floor AHU chilled water valve and later applied to the other three floors. All four original PI controllers had gains of pg = 1000 and ig = 20 with sampling times of $t_s = 1$ s, which are the recommended LOOP gains from [18]. As a starting point, the inner loop gain was set at a conservative value $k_L = 0.5$ and the outer loop gains at $k_{pc} = 1$ and $k_{ic} = 0.04$. When converted to nominal gains using the relationships of Equation (5), the resulting LOOP gains are equal to the original PI LOOP gains. This choice should provide similar transient performance to the original control, but with the added linearization benefits of the inner loop control. The resulting control gains (pg_c and ig_c) used in Algorithm 2 are calculated using Equation (8). The inner loop bias is the average of the minimum and maximum valve position (i.e., $B_2 = 50\%$). The outer loop bias is the average of the minimum and maximum allowable exit/discharge air temperatures, 52 °F and 65 °F, respectively. The overall bias term B for the PPCL code is therefore given by Equation (9), where DAT is discharge air temperature. Note that the bias term of the LOOP command has no scaling factor. Inner loop gains for all units were later increased to $k_L = 1$ starting in March 2018 to increase the level of cascaded linearization.

$$\text{pg}_\text{c} = 1000 k_L k_{pc} = 500 \quad \& \quad \text{ig}_\text{c} = 1000 k_L k_{ic} = 20, \tag{8}$$

$$\begin{aligned} \text{B} &= B_2 + k_L(\text{DAT} - B_1) \\ &= 50\% + \left(0.5\tfrac{\%}{^\circ\text{F}}\right)\left(\text{DAT} - \tfrac{65^\circ\text{F}+52^\circ\text{F}}{2}\right) \\ &= 20.75\% + \left(0.5\tfrac{\%}{^\circ\text{F}}\right)\text{DAT}, \end{aligned} \tag{9}$$

Building 0474 operations were transferred to a new server in the spring of 2017 with full historical trending of relevant HVAC operating points beginning approximately 1 August at 5 min intervals. Table 1 gives the results of analyzing each floor's AHU operation for fan and chilled water valve hunting with PI control through 31 December 2017. Overall, CHW (Chilled Water) control in Building 0474 displays very little hunting behavior except for the third floor where the valve hunts just over 10% of its operating time. Observations of building performance show that identified hunting in AHU3 occurs almost entirely in low cooling conditions. This indicates that the PI controller was likely tuned for mid-to-high load conditions. Hunting results for the CHW and fan control show that implementing cascaded control reduced hunting in the third-floor unit and had minimal effect on the other floors.

Table 1. Building 0474 Hunting Analysis Results with green arrows showing improvements and red arrows showing decline when compared to the PI control baseline case.

Control	Type	AHU1	AHU2	AHU3	AHU4
CHW Valve	PI	2.29%	1.05%	11.4%	2.12%
	Cascaded	↓1.91%	↑3.79%	⇊6.32%	↑3.35%
Fan Speed	PI	2.78%	0.17%	0.32%	0.52%
	Cascaded	↓1.24%	↓0.02%	↑0.42%	↓0.40%

The main benefits of cascaded control implementation at Building 0474 were improved tracking performance due to more aggressive performance afforded by the cascaded architecture. To fairly compare HVAC performance before and after implementation, weather disaggregation was applied to the data using the Degree Day (DD) method. A DD is related to how long and by how much outside ambient conditions stay above or below a baseline or balance temperature. Usually assumed to be 65 °F, this balance temperature is the ambient load condition under which a building requires no conditioning. Cooling and heating degree days, CDD and HDD, respectively, can be thought of as the area above or below the balance temperature for a given outside temperature profile. The DD is therefore a useful tool to compare HVAC data as it inherently normalizes for warmer or colder weather.

System performance is measured using the Root-Mean-Square (RMS) error given by Equation (10). For error to be calculated, the system must be ON and in cooling mode for more than 90 min. These criteria are important because, particularly on weekends, AHUs will cycle ON/OFF randomly for short periods of time to maintain building air quality. These bursts are not long enough for the AHUs to reach their setpoints and are not representative of the tracking ability of the valve controller. Detecting cooling mode is important as the chilled water valve can be saturated at 0% causing large error accumulation despite not being utilized. Criteria for detecting these conditions are given in Table 2 with cooling time found by the intersection of ON time and the negation of HEAT detection.

$$RMSE = \sqrt{\frac{\sum_{k=1}^{N}(T_{set}(k) - T(k))^2}{N}} \tag{10}$$

Table 2. Cooling Mode Detection Criteria for Building 0474.

Condition	Criteria	Comment
ON/OFF	$\omega_i = 0$ (Fan Speed)	Minimum ω_i when LOOP is active is 20%.
HEAT	$\delta_i = 0$ (Valve Opening)	Identified when true continuously for 90 min.

Improvements in system performance can be seen in Figure 7 that shows PI control data from 2017 and Cascaded Control (CC) data from 2018. For each floor, at least marginally, there is a reduction in dependence on load condition (i.e., flatter trend lines) and a much tighter dispersion of daily error with cascade control than PI control. This is seen visually and in the decrease in standard deviation from the trend line. Improved RMS error results show that the cascaded controller is better able to track setpoint changes and ensure occupant comfort.

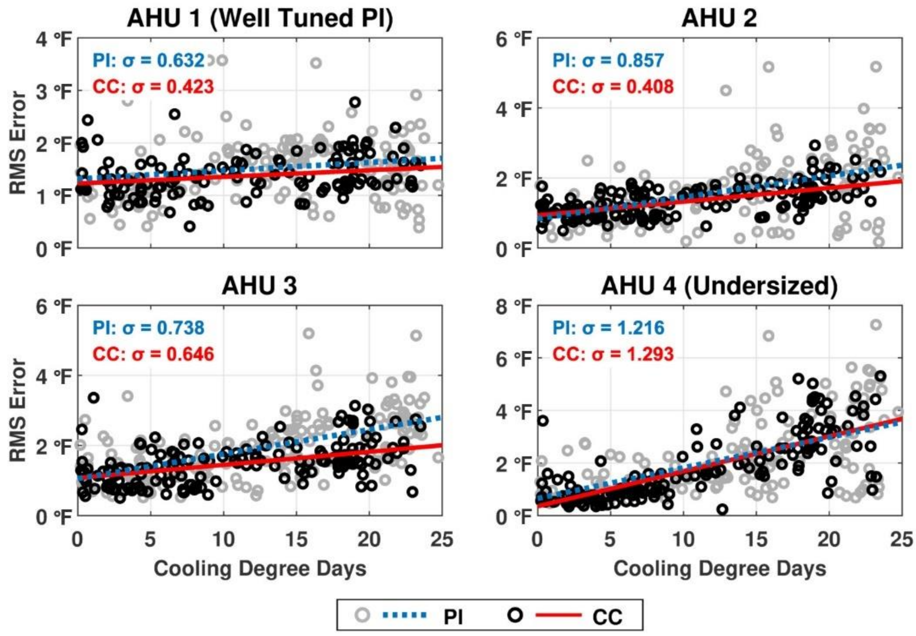

Figure 7. Performance comparison between PI and cascaded controllers at Building 0474. Cascaded control can be seen to provide tighter and more consistent performance.

The minimal improvements in AHU 1 and AHU 4 are the results of two main issues. For AHU 1, PI data from 2017 has less cold weather than CC in 2018. As these conditions tend to result in more error for this unit, the 2017 trend line is lower in this regime than expected. AHU 4 data is the result of the unit either being slightly undersized for observed loads or a system fault that restricts cooling capacity. In warm weather, AHU 4 was at maximum load with the valve and supply fan both operating continuously at 100%, but only slowly reaching command setpoints for static pressure and air temperature after several hours. This leads to large errors in warm weather that will be similar for both PI and CC control. However, there does appear to be an improvement in performance in cooler conditions. Overall, cascaded control was applied successfully to all AHUs at the YMCA building and showed performance benefits without introducing control hunting issues.

3.3. Building 1600 Results

Building 1600 is an approximately 85,000 ft^2 (7897 m^2) office and research facility completed in 1999 and consisting of three floors in a mostly L-shaped configuration with additional space on the ground floor. Each floor has a dedicated AHU and is numbered for the floor level it covers. AHU1, AHU2 and AHU3 have 63, 59, and 60 ton capacity with 22,050, 21,610, 20,160 CFM air flow capacity, respectively. There are 32 heating and cooling zones on the first floor, 40 on the second and 38 on the third floor roughly corresponding to the HVAC diagram given in Figure 8. Building 1600 has a 49 ton capacity Dedicated Outdoor Air System (DOAS) for its ventilation requirements that is functionally the same as a standard AHU except that 100% of its supply air is drawn from the outside (Figure 9). The DOAS supplies preconditioned ventilation air at maximum 7910 CFM to AHUs on each floor that have local cooling coils to make up for latent heat in the return air stream. Parallel fan powered VAV terminal boxes in each zone have reheat capabilities if necessary.

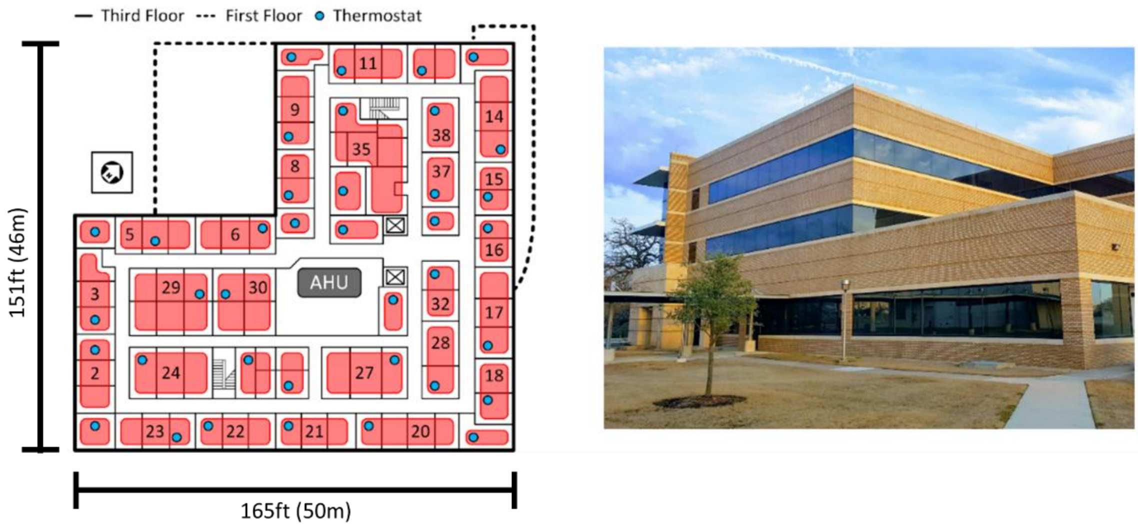

Figure 8. Layout of HVAC zones and exterior of Building 1600.

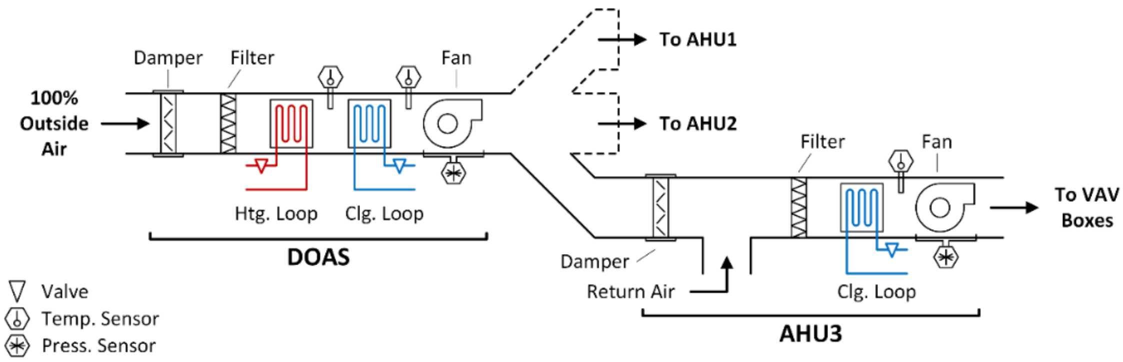

Figure 9. Building 1600 uses a dedicated outdoor air unit for ventilation supply to each floor's AHUs.

Historical data for this building was not available due to software limitations. However, dynamic trending of critical points for several months was facilitated by the university utilities office. This method of data collection records point values when signals vary above a threshold value with a maximum sampling time of 2 min. Data was initially collected from approximately 10:00 a.m. to 4:00 p.m. from November through December 2017 to capture original building operations. The nature of dynamic trending resulted in data sets with random sampling times. To utilize the hunting algorithm from [2], each dataset was resampled to enforce a 2 min sampling time.

Though Building 1600 is less than 20 years old and has an advanced HVAC system design, the AHU chilled water valve controls still have significant hunting issues. As seen in Figure 10, each floor's AHU valve control experiences some level of hunting behavior. AHU1 has a hunting period of approximately 60 min, AHU2 30 min, and AHU3 20 min. The level of hunting, in terms of amplitude and period, is again correlated with system load as it is significantly reduced/disappears when outdoor air temperature approaches 70 °F (21.1 °C). Apparent from the figure is the supply air fan for AHU2 also has a significant hunting issue. Fan speeds are allowed to vary within $\omega \in [20\%, 100\%]$ which accounts for the saturated appearance of the signal. Fan speeds for AHUs 1 and 2 vary only slightly or are constant during a normal day.

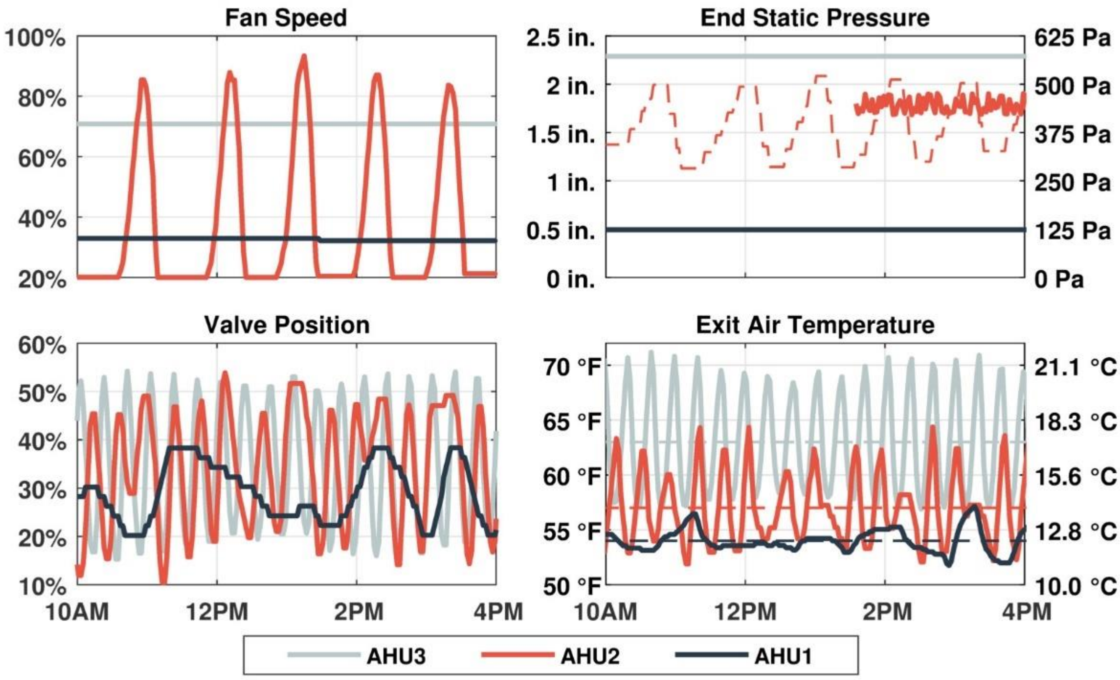

Figure 10. Performance data for Building 1600 on 5 December 2017 under original PI control shows significant levels of valve and fan hunting.

The tuning process at Building 1600 highlights several fundamental issues of practical building control. In particular, how hunting controllers can mask multiple system faults. The following sections detail issues discovered as they arose and how implementing cascaded control revealed the underlying problems.

3.3.1. Problem 1—Poorly Tuned Control Gains

Parsing building control code, the chilled water LOOP command settings for each AHU were found to vary widely as seen in Table 3. At issue are the vastly different sampling times seen in the upper floors. Due to the multiplication of the integral gain and sampling time (see Equation (4)), the effective integral gain for these systems is 30 times larger for upper floors than the first floor. Differences in gains help to explain the variation in loop performance between AHUs. Most likely, hunting behavior was observed in AHU3 and to compensate the magnitude of pg was reduced by an order of magnitude. Similarly, the integral gain for AHU1 was reduced to avoid oscillations.

Table 3. PI Control gains for Building 1600 AHU chilled water valves.

Unit	pg	ig	t_s (sec)	k_p	$k_i t_s$
AHU1	600	7.5	1	0.6	0.0075
AHU2	600	15	15	0.6	0.225
AHU3	60	15	15	0.06	0.225
DOAS	600	20	1	0.6	0.020

The main culprit of the nearly constant hunting in the initial dynamic data is therefore the large effective integral gains. From building data, however, there is still a clear dependence on operating conditions as warmer ambient temperatures reduce the prevalence of hunting. Implementing a properly tuned cascaded controller will therefore inherently eliminate oscillations due to poor tuning as well as reduce variations in performance due to changing operating conditions.

For initial cascaded tuning, the LOOP sampling time was $t_s = 1$ s with an initial inner loop gain of $k_L = 0.5$. The gains pg and ig for AHU1 were used as initial gains for the tuning process. The cascaded loop gains were therefore $k_{pc} = 0.2$ and $k_{ic} = 0.015$, which correspond to the initial LOOP gains $\mathrm{pg_c} = 100$ and $\mathrm{ig_c} = 7.5$ used with Algorithm 2. These calculations, including for the LOOP bias term, are given by Equations (11) and (12).

$$\mathrm{pg_C} = \mathrm{pg} - 1000k_L = 600 - 1000(0.5) = 100 \qquad \& \qquad \mathrm{ig_c} = \mathrm{ig} = 7.5, \tag{11}$$

$$\mathrm{B} = \mathrm{B}_2 - k_L\mathrm{B}_1 = 50\% - \left(0.5\frac{\%}{^\circ\mathrm{F}}\right)\left(\frac{65\ ^\circ\mathrm{F} + 55\ ^\circ\mathrm{F}}{2}\right) = 20\%, \tag{12}$$

After some initial testing, the inner loop gain was increased to $k_L = 1$ to amplify the linearization effect of the cascaded controller. Due to the additional issues discussed below, the integral gain was slowly decreased to $\mathrm{ig_c} = 2.5$. With these gains, the system showed a qualitative improvement in performance as seen in Figure 11. This improvement represents incremental progress with notable reductions in oscillation period and magnitude. After the remaining issues were fixed, the final integral gains for each unit were increased to 7.5, 10, 10, and 7.5, respectively.

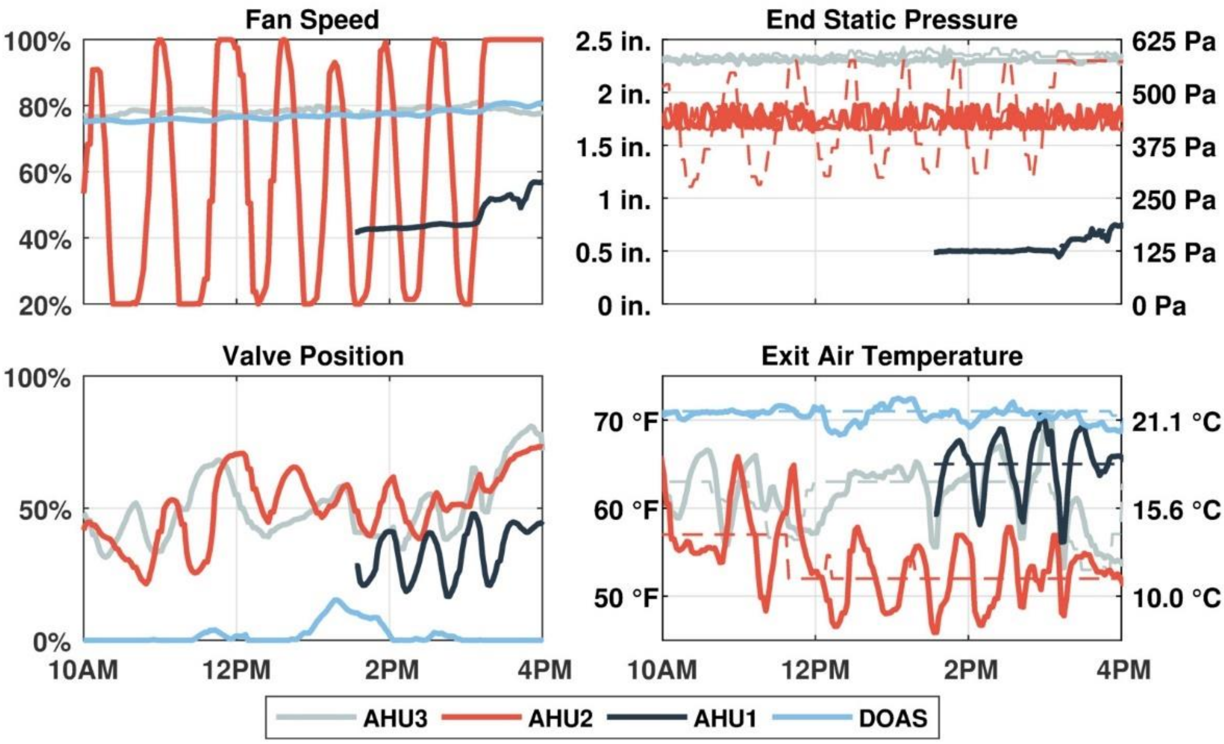

Figure 11. Performance data for Building 1600 on 20 March 2018 after initial cascaded loop tuning. Performance is improved but a fault with end static pressure sensors for AHU2 is exposed.

3.3.2. Problem 2—Failed End Static Pressure Sensors

As seen in Figure 11, fan speed for AHU2 hunts periodically throughout a normal day. The architecture of Figure 3 shows that the fan speed is used to maintain a certain static pressure at given points in the system ducting. Usually End Static Pressure (ESP) sensors are located at a point two-thirds along the longest path of the ducting. Given the L-shape of Building 1600, floors 2 and 3 have two ESP sensors.

In normal operation, the building code takes the minimum reading from the two ESP sensors as the input to the static pressure control loop. However, on floor 2 both sensors had failed, outputting a constant value that did not change with changes in supply fan speed. This had the effect of breaking the ESP feedback loop at the red mark shown in Figure 3, effectively introducing a constant disturbance between ESP setpoint and the fan speed control. While unmeasurable from the failed ESP sensors, the effect of the hunting fan speed was still observable through the damper command calculation. As dampers at each zones VAV box closed to accommodate rising ESP due to the increased fan speed, the ESP setpoint controller would lower the ESP setpoint. This process would reverse and eventually cause the observed sustained oscillation in the ESP setpoint. As soon as ESP sensors on floor 2 were replaced, the oscillations in AHU2 fan speed was eliminated giving the slightly improved results of Figure 12. Note that although AHU2 is parallel to AHU1 and AHU3, the hunting fan speed acted as a disturbance, affecting the distribution of fresh air being delivered to every AHU.

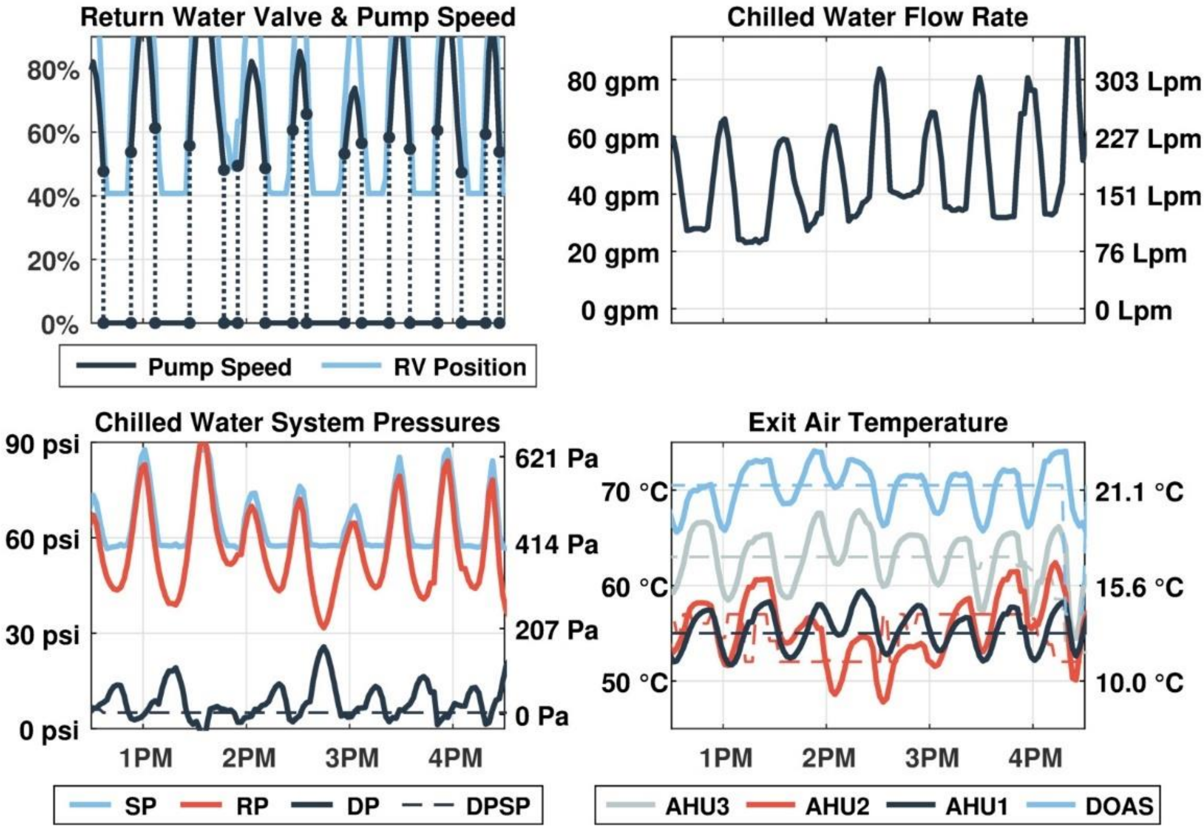

Figure 12. Data from Building 1600 on 16 April 2018 shows synchronized oscillations in AHU discharge air temperature due to short cycling of the building CHW pump, simultaneous actuation of the pump and the building return water valve, and a failed return water pressure sensor (RP).

3.3.3. Failed CHW System Pressure Sensor and Control Issue

After fixing the ESP sensor, a synchronized oscillation in all four AHUs in Building 1600 began to manifest (see Figure 12). Due to the configuration of the system, an issue with the DOAS was suspected as oscillations in discharge air temperature for that unit could propagate to the other three units. Trouble shooting proved inconclusive as simple valve stiction tests such as [19] failed to positively identify the issue.

In early April 2018, local weather conditions were cold enough that no conditioning of fresh air was needed from the DOAS. Despite the stable supply fresh air temperature being delivered to AHUs 1–3, discharge air temperatures still displayed the same synchronized oscillations. Their persistence strongly indicated that another upstream disturbance besides the DOAS was causing the oscillations.

Such a disturbance was determined to be coming from the building chilled water (CHW) supply system. As seen in Figure 13a, the system consists of two actuators (a pump and a valve) and sensors to measure Differential Pressure (DP). The CHW controller seeks to maintain a Differential Pressure Setpoint (DPSP) between the building supply and return water lines. DPSP is determined through a rule set that uses a time averaged Root-Mean-Square (RMS) valve position from the four AHUs. A PI controller operates on DP error to output DPLOOP $\in [20, 100]$, a demand variable that is interpolated to determine settings for the return water valve position and pump speed. A deadband block in the pump control is meant to prevent short cycling of the pump and to ensure that the pump and valve are actuating separately.

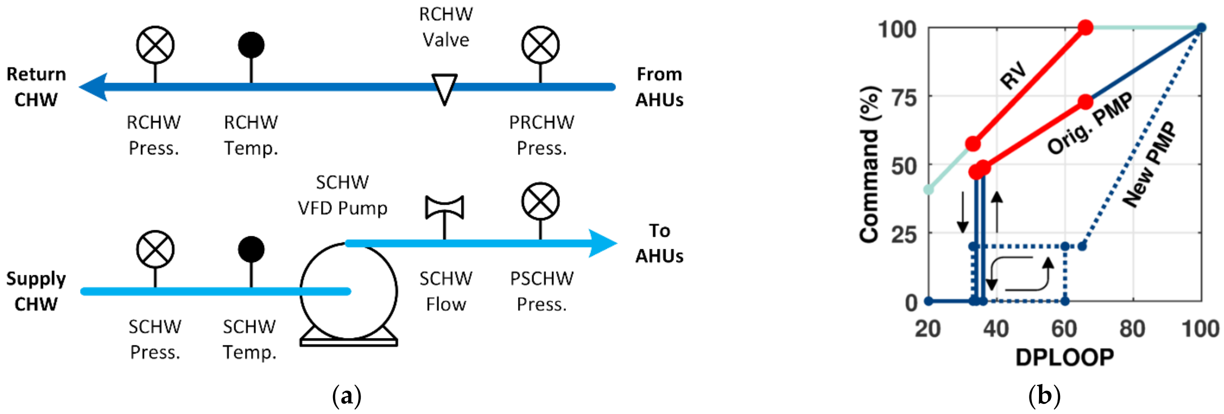

Figure 13. (**a**) Schematic of Building 1600 CHW supply system; (**b**) Comparison of original and new CHW system pump and valve control. Actuation overlap of return water valve and pump control (shown in red) resolved by adjusting deadband settings.

As seen in Figure 12, the building CHW pump short cycles ON/OFF several times throughout the day. These cycles correspond to the periodic oscillations seen in AHU discharge air temperature. The sudden changes in pump speed cause sharp changes in building CHW flow rate which affects flows to each individual AHUs simultaneously. The short cycling was due to several concurrent system issues. Firstly, the deadband region meant to prevent rapid pump cycles was extremely small turning ON the pump when DPLOOP rose above 36 and OFF when it dropped below 34. As DPLOOP would drop below 34 almost immediate after the pump switched ON, the pump would cycle OFF after the five-minute sampling time of the DPSP rules block. Additionally, because the linear interpolation for the return water valve was for $20 \leq \text{DPLOOP} \leq 66$, both the pump and the valve were actuating simultaneously for a significant range of operation shown graphically in Figure 13b. Secondly, the return CHW pressure (RP) sensor had a fault causing large swings in measurements. The resulting oscillation was propagated through the supply CHW PI controller causing the pump and valve to oscillate. Finally, the integral gain in the SCHW (Supply Chilled Water) PI loop was $\text{ig} = 125$ with a sampling time $t_s = 1$. The large integral gain caused DPLOOP to hunt even for small errors in DP. Each of these identified issues was fixed by working with campus utilities. The CHW program was changed to expand the deadband zone and alter interpolations to regions where the pump and valve actuate separately (see Figure 13b). The return pressure sensor was also replaced and calibrated and the DPLOOP PI controller was returned.

After fixing CHW supply issues, the system began to operate fault free. Initial results showed that hunting had been completely eliminated and that large disturbance oscillations due system faults had been removed. However, tracking performance was poor as cascaded controllers had been detuned to tolerate the many system faults. After retuning the controllers to improve tracking performance, system results are similar to those from Figure 14. Comparing with the original performance seen in Figure 10, implementing cascaded control and fixing the multiple faults revealed by the improved chilled water valve control has significantly improved building performance. Note that at the end of the tuning process, final cascaded LOOP gains were $k_L = 1$, $\text{pg}_c = 100$, and $\text{ig}_c = 10$ except for the DOAS whose integral gain was $\text{ig}_c = 7.5$.

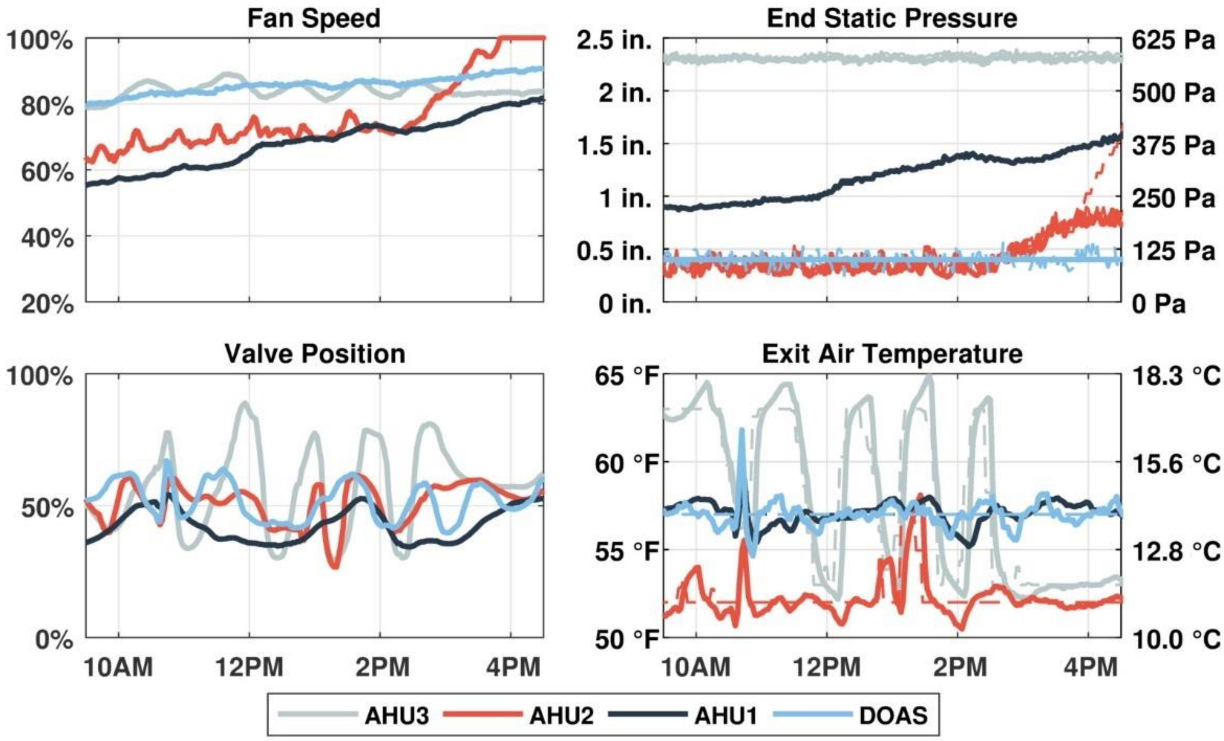

Figure 14. Data from Building 1600 on 14 May 2018 shows greatly improved building AHU discharge air temperature control due to cascaded control implementation and fixing revealed system faults.

4. Discussion

Having established that cascaded control can significantly improve the performance of AHU exit air temperature controllers, one final question is where the costs due to poor AHU valve control originate. The hidden and measurable costs of hunting behavior will be reviewed in this section, and the measured cost savings from the elimination of hunting results will be quantified.

4.1. Increased Replacement Costs

Most literature asserts that hunting will cause excessive component wear, eventually leading to increased replacement costs. While true, this cost is hard to estimate and is likely small because it only accounts for lost operation time as replacement actuators would be purchased regardless of hunting behavior.

4.2. Retuning Costs

Retuning costs due to occupant discomfort from hunting behavior are more easily estimated. Eliminating the time and expense of sending technicians to recommission each AHU on a seasonal basis has the potential for large savings in labor costs. However, such costs may vary across time and locations. In order to show the time-invariant effect of cascaded control, this paper will focus on quantifying the energy saving costs that require almost no investment costs.

4.3. Increased Energy Costs

There are additional energy costs associated with hunting behavior. Due to the nonlinear power consumption of most HVAC actuators (e.g., fan/pump power is cubically related to speed), more power is consumed above a nominal input than below. Thus, for oscillating signals, the average power consumed is greater than for the corresponding fixed signal.

This section quantifies the additional energy costs due to hunting behavior and the corresponding savings from the improved performance due to the implementation of cascaded controllers. As discussed in the previous section, equipment corrections at Building 1600 from the previous section have resulted in the HVAC system operating fault-free, and a comparison of daily energy usage and costs can be made by alternating between the original PI and new cascaded controllers. As the only difference will be the AHU temperature control architecture, assuming similar loads, any differences in energy usage are due to control type alone.

To estimate daily resource consumption, additional information about the building HVAC system was collected. The nominal power of the four AHU fans and CHW pump are known and given in Table 4. Each of these motors are variable speed, normally operating at some fraction of their maximum speed. The part load power can be found using standard fan/pump affinity laws leading to the instantaneous electrical power estimate of Equation (13) where $\omega_i \in [0, 100]$ are speeds and the subscripts '*oa*' and '*p*' are for the DOAS fan and SCHW pump, respectively. Each building on campus is billed at a rate of approximately 0.08 USD/kWh of electricity which represents the average cost of electricity production at the campus generation sites.

$$P_{elec} = 18.65\omega_1^3 + 18.65\omega_2^3 + 14.92\omega_3^3 + 5.595\omega_{oa}^3 + 14.92\omega_p^3 \qquad [\text{kW}] \tag{13}$$

Table 4. Building 1600 HVAC Motor List.

Unit	AHU1	AHU2	AHU3	DOAS	SCHW
Type	Fan	Fan	Fan	Fan	Pump
Power	25 HP	25 HP	20 HP	7.5 HP	20 HP

The volume of chilled water used daily by the HVAC system in Building 1600 is monitored in real time. However, the associated costs must be estimated since campus utilities does not bill by volume, but by energy content. As all conditioning water is returned to the central processing plants, buildings that require more cooling will return warmer water. Solely billing on volume usage therefore does not capture the additional cost of re-cooling warmer return water. Calculating energy used by the HVAC system requires monitoring chilled water flow rate as well as the temperature differential between supply and return water. The instantaneous power delivered by the CHW is given by Equation (14).

$$P_{CHW} = c_p\,\rho\,\dot{V}\,\Delta T = 0.1463\,\dot{V}\,\Delta T \quad [\text{kW}] \tag{14}$$

This estimated power does not include costs associated with chilled water production. An estimate for production cost is found by assuming an efficiency from a comparable air-cooled chiller system. Coefficient of Performance (COP) curves for such a system are shown in Figure 15a, based on the model from [20]. The chiller was sized at 400 kW using the 98th percentile of instantaneous chilled water power observed for the period between May through December of 2018. This assures that the unit will meet almost all demand by the building chilled water system with nominal operation in a region of high COP. To calculate the chiller electric power, Equation (15) divides the instantaneous chilled water consumption by a cubic interpolation of the chiller COP based on part load (L_p) and outdoor air temperature (T_{oa}).

$$P_c = \frac{P_{CHW}}{\text{COP}\left(L_p, T_{oa}\right)} \tag{15}$$

The COP curves shown in Figure 15a are used to estimate the additional costs associated with oscillations in chiller load. As discussed previously, hunting results in above average energy use for systems with nonlinear power profiles. Thus, for the chilled water, the additional cost of hunting is expected to be greatest in the regions where COP surface is the most nonlinear. However, hunting is most prevalent in times where the system part load is low (i.e., in cool weather with minimal demand). The COP curve in that region is essentially linear indicating that there will be minimal wasted energy due to hunting oscillations. To illustrate this effect, the cost penalties for a sinusoidal chilled water demand (5% variation around the nominal load) are given in Figure 15b, which shows wasted energy in the region of interest to be between 0.05 and 0.1%. This level of wasted energy might seem insignificant. However, a 5% variation around nominal load is a conservative estimation, and ±20% or more variation can often be observed (see Figures 10 and 11). Additionally, Figure 15b shows a sharp increase in wasted energy when the outside temperature is low, and the load is high. Systems tuned for high temperatures can suffer significantly with exacerbated level of wasted energy.

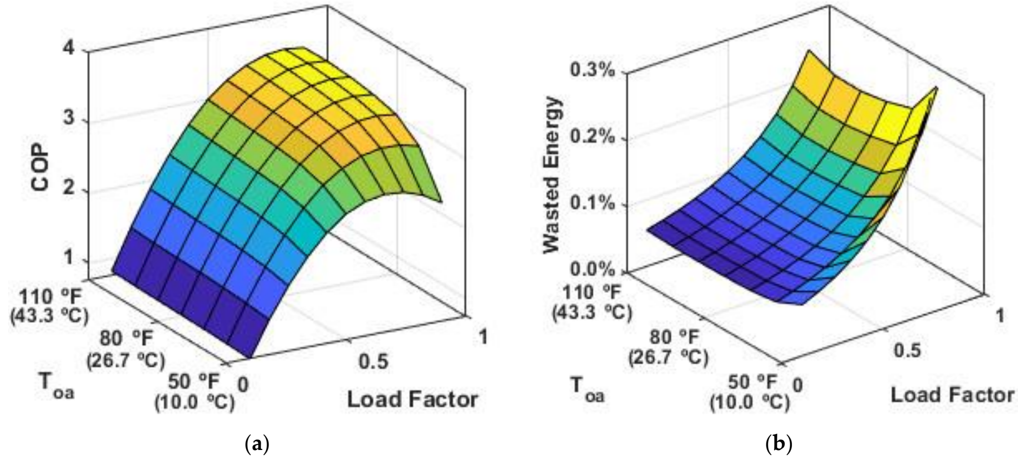

Figure 15. (**a**) COP surface for a rooftop air-cooled chiller system; (**b**) Estimated wasted energy due to ±5% sinusoidal hunting chiller load factor.

4.4. Estimated Cost Savings at Building 1600

The AHU discharge air temperature control (i.e., valve control) was switched between the original hunting PI control and the new cascaded control approximately every two weeks from May 2018 through May 2019. Leverage and standardized residual methods were used to filter outliers from daily data and to ensure a consistent comparison of the two approaches. More details on the statistical method used for the outliers can be found in Appendix A. Energy consumption, costs, and cooling degree days were calculated daily to generate Figure 16, comparing the two control architectures.

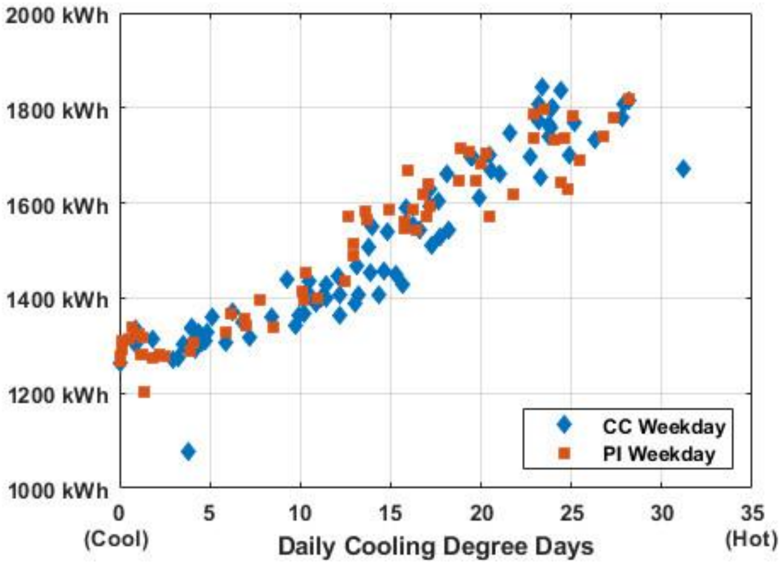

Figure 16. Daily HVAC energy production and usage costs for Building 1600 from May 2018 through May 2019.

Analysis of the two data sets (i.e., energy use with PI control and cascaded control) found statistically significant differences in bias values but not slopes. Equation (16) shows a difference of 54.6 kWh in daily AHU energy consumption for models fit with a constraint on equal slopes. The smaller intercept value for the cascaded controller indicates that it is better able to eliminate oscillatory behaviors that result in wasted energy and can better follow setpoints due to faster transient responses. The reduced bias value corresponds to a 2.2–4.4% savings in total energy consumed by the AHU system. This analysis, however, does not include other important cost factors of hunting. The true costs of hunting behavior would also include an increase in maintenance costs, resulting from the frequent actuation. When the maintenance and energy savings are combined with the economical and ease of implementation, cascade control in buildings is strongly recommended.

$$\begin{aligned} E_{PI} &= 1488.3 + 35.8 \times CDD \quad [\text{kWh}] \\ E_{C} &= 1393.7 + 35.8 \times CDD \quad [\text{kWh}] \end{aligned} \tag{16}$$

5. Conclusions

Hunting behavior in buildings causes an increase in operating cost arising from: (1) increased replacement frequency of components due to excessive component wear, (2) retuning cost due to occupant discomfort, and (3) increased energy cost. Among these costs, this paper has focused on quantifying the energy savings from the detection and elimination of hunting behavior in several buildings on a university campus through the implementation of cascaded control loops. Shown in Figures 4 and 5, hunting in Building 1497 valve was significantly reduced from cycling 10 to 20 times per hour to no oscillations after the cascaded control implementation. As a result, exit air temperature that used to vary more than 2 °F was reduced within 0.5 °F. Shown in Figures 10 and 14, valve hunting in Building 1600 AHU2 and AHU3 decreased, with oscillations in valve position decreasing in magnitude from 30% to 20% after the implementation of cascaded control. Additionally, the actuation frequency decreased from approximately 3 to 4 cycles per hour to 1 cycle per hour for AHU3 and AHU2. Results at Building 0474 were mixed with a slight improvement in tracking performance but an overall improvement in the consistency of AHU discharge air temperature regulation. An estimation of the costs of poor AHU discharge air temperature control was presented for Building 1600. These results show 2.2–4.4% energy cost savings due to the elimination of chilled water valve hunting, with further potential savings associated with reduced maintenance costs. Further work and detailed analysis can be found in [4].

Results also show the mechanism for hunting behavior to cause a more measurable loss of efficiency in HVAC systems. While chilled water production may have minimal nonlinearity around a given operating point, fan and pump affinity laws have a consistent nonlinear relationship between speed and power. Should hunting be induced in those actuators due to their poor control or that of an upstream controller (i.e., chilled water control), energy savings will be more prevalent. This paper has shown that cascaded control improves tracking performance, reduces the need for seasonal retuning due to its inherently non-linearity limiting nature, and is easy to implement with a single LOOP command. While the scope of this paper has been on improving supply water control, many campus buildings examined by the authors have shown hunting behavior in their AHU supply fan loops. Implementation of cascaded control loops at these buildings can be used to more easily establish energy penalties related to poor PI control design.

Author Contributions: Conceptualization and research supervision, B.P.R.; methodology and investigation, C.P.; analysis and data curation, C.P. and D.P.; writing—original draft preparation, C.P.; writing—review and editing, C.P., B.P.R. and D.P. All authors have read and agreed to the published version of the manuscript.

Funding: This research was funded by National Science Foundation, grant number CMMI-1563361.

Data Availability Statement: Not applicable.

Acknowledgments: Special thank you to the Building Automation Supervisor, Christopher Dieckert, and the Texas A&M University Utilities and Energy Services for their support in conducting this research.

Conflicts of Interest: The authors declare no conflict of interest.

Nomenclature

B	Bias
C	Cooling demand
c_p	Heat capacity
CDD	Cooling Degree Day
COP	Coefficient of Performance
D	Damper demand
e	Error
E	Energy
F	Flow demand
G	System transfer function
k	Control gain
L	Inner loop transfer function
L_p	Part load
P	Power
PID	Proportional-Integral-Derivative controller
r	Reference input (set point)
$RMSE$	Root-Mean-Square error
s	Laplace variable
t	Time
u	Control signal
$\dot{V}$	Volumetric flowrate
y	Output
δ	Valve opening
θ	Damper position
ρ	Density
σ	Operating condition
ψ	Nonlinear gain
ω	Rotational speed
Subscripts	
C	Cascaded
CHW	Chilled water
D	Derivative
$elec$	Electric
i, L	Inner loop
I	Integral
o	Outer loop
oa	Outside air
p	Proportional
pc	Proportional-cascade
PI	Proportional-Integral
s	Sample
set	Setpoint

Appendix A

A set of linear regressions can be generalized into a matrix representation as in Equation (A1). Based on the regression fit, prediction of dependent variables can be accomplished using Equation (A2). With matrix manipulation, prediction can be expressed in terms of observation y as in Equation (A3). The matrix H can then be defined and maps the observation y to the prediction $\hat{y}$ as in Equation (A4).

$$Y = X\beta + e, \tag{A1}$$

$$\hat{y} = Xb, \tag{A2}$$

$$\hat{y} = X(X'X)^{-1}X'y, \tag{A3}$$

$$\hat{y} = Hy, \tag{A4}$$

The diagonal elements in the H matrix are called leverage points. These points represent the effect of observation y_i on prediction value $\hat{y}_i$. Points with high values of leverage points can be labeled as outliers and be filtered out. Another way to define leverage point is shown in Equation (A5). With expressions for the leverage points defined, a general rule-of-thumb of filtering criterion for leverage is presented in Equation (A6).

$$h_{ii} = \frac{1}{n} + \frac{(x_i - \overline{x})^2}{\sum_{j=1}^{n}(x_j - \overline{x})^2}, \tag{A5}$$

$$h_{ii} > \frac{6}{n}, \tag{A6}$$

As a second set of filters, the standardized residuals method was used to further process the building data. Standardized residual is defined as the ratio of the prediction error, e_i, over the standard deviation of the error (Equation (A7)). Points with standardized residual magnitude above 95% percentile confidence level of t distribution outlined in Equation (A8) were labeled as outliers and filtered out, where n is number of observations and k is the number of predictors.

$$e_i^* = \frac{e_i}{sd(e_i)}, \tag{A7}$$

$$t(n-k-2), \tag{A8}$$

After the outliers had been removed, analysis of covariance was conducted to separate out the covariate effect of cooling degree days on the dependent variable, total energy consumption. In the analysis of covariance, cascade and PI control are classified by $\lambda = 1$ and $\lambda = 0$, respectively. In the analysis of data, the two different control algorithm distributions are fitted to one of the following cases:

Case I: Different intercepts and different slopes

$$Y = \beta_0 + \beta_1\lambda + \beta_2 X + \beta_3\lambda X + e, \tag{A9}$$

Case II: Different intercepts but same slopes

$$Y = \beta_0 + \beta_1\lambda + \beta_2 X + e, \tag{A10}$$

Case III: Same intercepts and same slopes

$$Y = \beta_0 + \beta_3 X + e, \tag{A11}$$

Data from Building 1600 was used to test which of these cases best fit the results. Using Case I, Table A1 is generated. For Case I, β_3 had high p-value and therefore, the two data sets have no significant difference in their slopes. Case II was checked for the two different controller data sets. p-values from Table A1 show significant differences in intercepts with same slopes. β_0 gives the intercept for the PI controlled dataset and $\beta_0 + \beta_1$ gives the intercept for the cascaded control dataset. Case III was not performed since Case II showed statical significance.

Table A1. Case I and II Fitted with Building Data.

Coefficient			t	$P > \|t\|$
Case I	β_1	−92.8	−2.947	0.004
	β_3	2.9	1.441	0.152
Case II	β_0	1448.3	-	-
	β_1	−54.6	−3.202	0.002
	β_2	35.8	-	-

References

1. Price, C.; Liang, S.; Rasmussen, B. HVAC Nonlinearity Compensation Using Cascaded Control Architectures. *ASHRAE Trans.* **2015**, *121*, 217–231.
2. Chintala, R.; Liang, S.; Price, C.; Rasmussen, B. Identification and Elimination of Hunting Behavior in HVAC Systems. *ASHRAE Trans.* **2015**, *121*, 294–306.
3. Hägglund, T. A Control-Loop Performance Monitor. *Control Eng. Pract.* **1995**, *3*, 1543–1551. [CrossRef]
4. Price, C.R. Cascaded Control for Improved Building HVAC Performance. Ph.D. Thesis, Texas A&M University, College Station, TX, USA, 2018.
5. Hou, Z.-S.; Wang, Z. From Model-Based Control to Data-Driven Control: Survey, Classification and Perspective. *Inf. Sci.* **2013**, *235*, 3–35. [CrossRef]
6. Desborough, L.; Miller, R. Increasing Customer Value of Industrial Control Performance Monitoring -Honeywell's Experience. *AIChE Symp. Ser.* **2002**, *98*, 169–189.
7. Blevins, T.L. PID Advances in Industrial Control. *IFAC Proc. Vol.* **2012**, *45*, 23–28. [CrossRef]
8. O'Dwyer, A. *Handbook of PI and PID Controller Tuning Rules*, 3rd ed.; Imperial College Press: London, UK, 2009.
9. Li, Y.; O'Neill, Z.D.; Zhou, X. Development of Control Quality Factor for HVAC Control Loop Performance Assessment I—Methodology (ASHRAE RP-1587). *Sci. Technol. Built Environ.* **2019**, *25*, 656–673. [CrossRef]
10. Price, C.; Rasmussen, B. Optimal Tuning of Cascaded Control Architectures for Nonlinear HVAC Systems. *Sci. Technol. Built Environ.* **2017**, *23*, 1190–1202. [CrossRef]
11. Elliott, M.S.; Estrada, C.; Rasmussen, B.P. Cascaded Superheat Control with a Multiple Evaporator Refrigeration System. In Proceedings of the 2011 American Control Conference, San Francisco, CA, USA, 29 June–1 July 2011; pp. 2065–2070.
12. Price, C.R.; Rasmussen, B.P. Effective Tuning of Cascaded Control Loops for Nonlinear HVAC Systems. In *American Society of Mechanical Engineers Digital Collection, Proceedings of the ASME 2015 Dynamic Systems and Control Conference, Columbus, OH, USA, 28–30 October 2015*; American Society of Mechanical Engineers: New York, NY, USA, 2016.
13. Guo, C.; Song, Q.; Cai, W. A Neural Network Assisted Cascade Control System for Air Handling Unit. *Ind. Electron. IEEE Trans.* **2007**, *54*, 620–628. [CrossRef]
14. Elliott, M.; Walton, Z.; Bolding, B.; Rasmussen, B. Superheat Control: A Hybrid Approach. *HVAC&R Res.* **2009**, *15*, 1021–1043. [CrossRef]
15. *Applications Guide PID Control in Tracer Controllers*; American Standard Inc.: Piscataway, NJ, USA, 2001. Available online: https://www.trane.com/Commercial/Uploads/Pdf/1007/CNTAPG002EN.PDF (accessed on 31 August 2022).
16. Yin, X.; Wang, X.; Li, S.; Cai, W. Energy-Efficiency-Oriented Cascade Control for Vapor Compression Refrigeration Cycle Systems. *Energy* **2016**, *116*, 1006–1019. [CrossRef]
17. Bengea, S.C.; Kelman, A.D.; Borrelli, F.; Taylor, R.; Narayanan, S. Model-Predictive Control for Mid-Size Commercial Building HVAC: Implementation, Results and Energy Savings. In Proceedings of the Second International Conference on Building Energy and Environment, Boulder, CO, USA, 1 August 2012.
18. *APOGEE Powers Process Control Language (PPCL) User's Manual*; Siemens Building Technologies, Inc.: Florham Park, NJ, USA, 2000.
19. Choudhury, M.A.A.S.; Kariwala, V.; Shah, S.L.; Douke, H.; Takada, H.; Thornhill, N.F. A Simple Test to Confirm Control Valve Stiction. *IFAC Proc. Vol.* **2005**, *38*, 81–86. [CrossRef]
20. Yu, F.W.; Chan, K.T. Optimizing Condenser Fan Control for Air-Cooled Centrifugal Chillers. *Int. J. Therm. Sci.* **2008**, *47*, 942–953. [CrossRef]